

Elsevier Editorial System(tm) for Earth and Planetary Science Letters  
Manuscript Draft

Manuscript Number: EPSL-D-12-00873R2

Title: Comment on « Displacement along the Karakoram fault, NW Himalaya, estimated from LA-ICP-MS U-Pb dating of offset geologic markers » published by Shifeng Wang et al. in EPSL, 2012.

Article Type: Commentary and Reply

Keywords: Kararakoram Strike-slip fault, Offset, dating deformation, rate, synkinematic melting

Corresponding Author: Dr. Philippe Hervé Leloup, Ph.D.

Corresponding Author's Institution: CNRS

First Author: Philippe Hervé Leloup, Ph.D.

Order of Authors: Philippe Hervé Leloup, Ph.D.; Roberto F Weinberg, Ph.D.; Barun K Mukherjee, Ph.D.; Paul E Tapponnier, Ph.; Robin Lacassin, Ph.D.; Emmanuelle Boutonnet, Ph.D.; Marie-Luce Chevalier, Ph.D.; Franck Valli, Ph.D.; Haibing Li, Ph.D.; Nicolas Arnaud, Ph.D.; Jean-Louis Paquette, Ph.D.

1 Comment on « Displacement along the Karakoram fault, NW Himalaya, estimated  
2 from LA-ICP-MS U–Pb dating of offset geologic markers » published by Shifeng  
3 Wang et al. in EPSL, 2012.

4  
5 P.H. Leloup (1), R.F. Weinberg (2), B. K. Mukherjee (3), P. Tapponnier (4), R.  
6 Lacassin (5), E. Boutonnet (1) (6), M.-L. Chevalier (7), F. Valli (8), H. Li (7), N.  
7 Arnaud (9), J.-L. Paquette (10).

8 1 Laboratoire de Géologie de Lyon, Université de Lyon, Université Lyon 1, ENS de Lyon,  
9 CNRS, 2 rue Raphael Dubois 69622 Villeurbanne, France.

10 2 School of Geosciences, Monash University, Clayton, Vic 3800, Australia

11 3 Wadia Institute of Himalayan Geology, 33, GMS Road, Dehra Dun-248 001, India

12 4 Tectonics Group, Earth Observatory of Singapore, Nanyang Technological University,  
13 Singapore.

14 5 Equipe de Tectonique, Institut de Physique du Globe de Paris, Sorbonne Paris Cité, Univ Paris  
15 Diderot, UMR 7154 CNRS, F-75005 Paris, France.

16 6 Institute of Geosciences, Johannes Gutenberg University Mainz, J.-J.-Becher-Weg 21 D-  
17 55128 Mainz, Germany.

18 7 State Key Laboratory of Tectonics and Continental Dynamics, Institute of Geology, Chinese  
19 Academy of Geological Sciences, Beijing 100037, China.

20 8 Newmont Mining Corporation, Perth Area, Australia.

21 9 Géosciences Montpellier, UMR CNRS 5243, Université de Montpellier 2, France

22 10 Laboratoire Magma et Volcans, UMR CNRS 6524, Université Blaise Pascal, Université de  
23 Clermont-Ferrand, France.

24

## 25 **Abstract**

26 Field evidence for syn-deformation migmatization and crystallization along  
27 the Karakoram fault contradicts the study of Wang et al. [2012]. The ages of such  
28 magmatic rocks provide minimum ages for the onset of deformation at ~23 Ma in  
29 North Ayilari and ~19 Ma in Tangtse. The onset of deformation at 12 Ma in the  
30 Ayilari range inferred by Wang et al. [2012] from a muscovite Ar/Ar age is a  
31 cooling age, thus only a minimum age. The ~60 Ma granodiorite bodies, the

32 ophiolitic rocks and the south Kailash thrust that are correlated across the fault to  
33 provide a  $52\pm 2$  km finite offset do not define reliable piercing points. Such  
34 observations as well as our previous work concur to show that the Karakorum  
35 fault initiated in the Oligo-Miocene, and has a long-term dextral slip-rate between  
36 7.5 and 13 mm/yr, approximately twice that proposed by Wang et al. [2012].

37

## 38 **Introduction**

39 Wang et al. [2012] published a high quality set of new U/Pb zircon ages  
40 from the Ayilari and Kunsha granites located across the Karakorum fault (KKF) in  
41 western Tibet. They confirm that both granites experienced crystallization events  
42 at  $\sim 60$  and  $\sim 50$  Ma, and that the North Ayilari granite (also called Zhaxigang)  
43 experienced a late crystallization event at  $\sim 20$  Ma. Based on this chronological  
44 data, and on consideration of other potential offset markers, they infer a finite  
45 offset of  $52\pm 2$  km on the KKF, dismissing previously proposed larger offsets.  
46 They propose that motion on the KKF initiated at  $\sim 16$  Ma in its central part at  
47 Tangtse (Ladakh, India), and propagated to the southeast to reach the Gar-Namru  
48 area (Ayilari range) by  $\sim 12$  Ma. They consequently calculate a slip rate of  $4.5\pm 0.1$   
49 mm/yr since 12 Ma. This is taken as evidence for Tibet deforming in distributed  
50 fashion rather than by localized strain through extrusion along major faults.

51 This debate on initiation age, total offset and slip rate of the KKF, which  
52 started 25 years ago, continues despite significant technical advances and much  
53 improved knowledge of this remote area [e.g., *Chevalier et al.*, 2005; *Lacassin et*  
54 *al.*, 2004a; *Murphy et al.*, 2000; *Peltzer and Tapponnier*, 1988; *Robinson*, 2009;  
55 *Searle*, 1996; *Searle and Phillips*, 2007; *Valli et al.*, 2008]. Wang et al. [2012]  
56 contribute to this effort by bringing new age constraints on granites located on  
57 both sides of the fault. Regrettably, they do not take into account key structural  
58 observations that must be considered in order to understand and constrain the  
59 deformation timing, offsets and displacement rates along the fault. We show  
60 below that the initiation age inferred by Wang et al. [2012] is based on an

61 erroneous assumption, and is incompatible with older ages of demonstrably  
62 synkinematic granites. We also argue that the piercing points the authors define  
63 are far from adequate to measure the total offset on the fault.

64

### 65 **Timing of right-lateral deformation along the Karakorum fault.**

66 Ductile mylonites related to the KKF have been described at three locations:  
67 Nubra Valley, Darbuk-Tangtse-Pangong region and North Ayilari range. In  
68 Tangtse, a key outcrop shows a mylonitic granitic dyke (sample P11) concordant  
69 to the foliation whose crystallization has been dated at  $15.87 \pm 0.08$  Ma and an  
70 undeformed cross-cutting dyke (sample P8) with an age of  $13.73 \pm 0.34$  Ma  
71 [Searle and Phillips, 2007 and references therein] (Fig. 1a). This was interpreted  
72 as bracketing the ductile deformation that would have lasted less than 2.2 Ma  
73 [Searle and Phillips, 2007 and references therein]. Because comparable dykes  
74 give similar ages in the Nubra Valley, and disregarding evidence for synkinematic  
75 partial melting in the granites and migmatites, the inference that most magmatism  
76 predates fault movement was extended from a single outcrop to the entire KKF  
77 [Searle and Phillips, 2007 and references therein]. Following this inference, Wang  
78 et al. [2012] assume without producing new evidence, that none of the granites of  
79 the Ayilari and Tangtse ranges are synkinematic and that the KKF must be  
80 younger than 16 Ma.

81 However, evidence for synkinematic melting and granite migration in the  
82 Darbuk-Tangtse-Pangong and North Ayilari regions are plentiful, and some of the  
83 data provided by Searle and Phillips [2007] are inaccurate. For example, their P8  
84 dyke, which is depicted as cross-cutting the whole KKF Tangtse mylonitic strand  
85 (Fig. 3 in [Searle and Phillips, 2007]), is in fact only 8 m-long and shows dextral  
86 deformation tails attesting that it is syntectonic (Fig. 1a & b). Other evidence for  
87 syntectonic magmatism are: 1) At a microscopic scale, late melt channels  
88 following two distinct orientations, are parallel to the S-C fabric resulting from  
89 right-lateral shear in the Karakorum Shear Zone (Fig. 1f), thus implying that

90 magma migration was coeval with deformation [Hasalova *et al.*, 2011]. 2) Dykes  
91 cross-cutting foliation but which are themselves deformed (e.g. P8, Fig. 1a,b;  
92 K1C32, Fig. 1e), [Boutonnet *et al.*, 2012; Valli *et al.*, 2008]. 3) Leucosome pods  
93 affecting the foliation but overprinted by right-lateral shearing (Fig. 1c & d)  
94 [Boutonnet *et al.*, 2012]. 4) Magmas formed by local anatexis and migrating  
95 during folding into axial-planar leucosomes, sub-parallel to the mylonitic foliation,  
96 indicating that anatexis, folding and right-lateral shearing were coeval [Weinberg  
97 *et al.*, 2009 and references therein] (Fig. 1h). 5) Leucosomes filling boudin necks,  
98 indicative of *in situ* partial melting during deformation [Mukherjee *et al.*, 2012]  
99 (Fig. 1g). 6) At a macroscopic scale, the close relationship between the dyke  
100 network and the structures resulting from right-lateral shear has led Reichardt *et*  
101 *al.* [2010] to propose that magma migration was controlled by stresses related to  
102 right-lateral transpression. 7) Last but not least, the  $18.5\pm 0.2$  Ma South Tangtse  
103 granite shows progressive transition from an undeformed granite in its central part,  
104 to a granite with faint magmatic foliation, and finally to a mylonitic orthogneiss  
105 along the Tangtse strand of the KKF, indicative of its syntectonic nature [Leloup  
106 *et al.*, 2011].

107         The ages of granitoids with robust structural evidence for syn-deformation  
108 crystallization are  $\sim 23$  Ma in North Ayilari [Valli *et al.*, 2008] and span between  
109  $\sim 19$  and 14 Ma in Tangtse [Boutonnet *et al.*, 2012], implying that the KKF  
110 deformation started prior to the Lower Miocene at these locations. Note that such  
111 observations neither imply nor necessitate magma generation to be due to strike-  
112 slip deformation.

113         Wang *et al.* [2012] take the  $12\pm 1$  Ma muscovite Ar/Ar age from sample A12  
114 within the KKF shear zone in the Ayilari range as reflecting the onset of  
115 deformation at this location although there is no clear evidence for such an  
116 interpretation. Indeed, Ar/Ar ages are acquired at or below the closure temperature  
117 of a mineral and do not alone provide an age for the initiation of deformation. In  
118 the case of the Ayilari range, microstructural evidence, such as feldspar core-and-

119 mantle structures and subgrain rotation deformation regime in quartz, indicate that  
120 deformation started at temperatures above 500°C [e.g. *Valli et al.*, 2008] while the  
121 closure temperature for Ar in muscovite is ~ 425°C. Thus, sample A12 Ar/Ar age  
122 only provides a minimum age for the onset of deformation.

123 We therefore argue that our previous conclusions that the KKF initiated  
124 prior to 19 Ma in Tangtse, 23 Ma in North Ayilari and 13 Ma in South Ayilari are  
125 more accurate determinations than Wang et al.'s suggestion.

126

### 127 **Amount of offset across the Karakorum fault.**

128 Wang et al. [2012] link the Namru ~60 Ma granodiorite body located  
129 southwest of the KKF (sample Z03, Fig. A1) with another ~60 Ma granodiorite  
130 body located across the KKF (samples K11 and K07, Fig. A1), in order to restore  
131 a 52±2 km right-lateral offset across the fault. However, granodiorite bodies of  
132 this age relate to the most voluminous magmatic pulse in the Ladakh and  
133 Gangdese batholiths and can be found all the way to the Lhasa region more than  
134 1000 km farther east [e.g., *Ji et al.*, 2009]. The challenge is thus to determine  
135 which ~60 Ma granodiorite body correlates with the Namru one. Matching  
136 granodiorite K13 results in a ~27 km left-lateral offset (Fig. A1) inconsistent with  
137 a right-lateral KKF. Matching any granodiorite body located north of the KKF and  
138 east of Menci yields a right-lateral offset larger than 52 km.

139 According to Wang et al. [2012], the proposed ~50 km offset is confirmed  
140 by a similar offset of rocks from the Yarlung-Zangbo (YZ) suture and of the Great  
141 Counter Thrust (GCT, locally called the South Kailash Thrust), two more  
142 distinctive markers. However, the trace of the KKF depicted in Wang's et al.  
143 [2012] Figure 4 is misleading: morphological and geological evidence show that  
144 the KKF bends eastwards and that its main trace lies north of the Menci basin,  
145 trending ~N120° north of the Raksas lake [Figs. 2, 8 & 12 in *Chevalier et al.*,  
146 2012; Figs. 7b & c in *Lacassin et al.*, 2004b], and that the South Kailash thrust is a  
147 transpressive branch of the KKF itself (Fig. A1). The northernmost ultramafic

148 rocks, including those taken by Wang et al. [2012] to define a piercing point  
149 because supposedly lying NE of the KKF, are in fact exposed in narrow slivers  
150 bounded by WNW-SSE splays of the KKF (Fig. A1). Such slivers show clear  
151 structural evidence for right-lateral shear [Figs. 7b & c in *Lacassin et al.*, 2004],  
152 and are thus best interpreted to lie within the KKF zone. The YZ piercing point  
153 thus only yields a minimum offset, with the KKF following the northern edge of  
154 the suture after having obliquely cut the batholith (Fig. A1).

155 Wang et al. [2012] consider the apparent offset of the GCT to constrain both  
156 the age (less than 12 Ma) and the total offset (~60 km) of the KKF. However, the  
157 EW striking GCT and the NW-SE striking right-lateral KKF are compatible with  
158 the same regional state of stress. The GCT may have formed at a time when the  
159 KFZ was already active, in which case it cannot be used to define the piercing  
160 points of a total offset. Furthermore, the Kailash thrust has been interpreted as part  
161 of a flower structure branching on the KKF [*Lacassin et al.*, 2004b] (Fig. A1).

162 A more detailed assessment of the most probable propagation timing and  
163 large-scale offsets of the KKF is beyond the scope of this comment. We refer to  
164 the detailed discussions in Valli et al. [2008] that favour a total offset of 200 to  
165 240 km, with an offset of ~120 km since ~14 Ma in the central section of the  
166 KKF. These estimates are based on the large-scale bending of the YZ suture, the  
167 offsets of the Late Cretaceous Shyok and Shiquanhe sutures, and the minimum  
168 dogleg offset of the Indus river. Corresponding long-term dextral slip-rates thus  
169 range between 7.5 and 13 mm/yr, approximately twice that proposed by Wang et  
170 al. [2012], but consistent with the Late Pleistocene rates derived from the offsets  
171 of dated moraines and fluvial surfaces by Chevalier et al. [2012].

172

### 173 **Conclusion.**

174 As opposed to what is asserted by Wang et al. [2012], there is compelling  
175 evidence for synkinematic migmatites and granites within the KKF zone. These  
176 granitic melts are the rocks that provide a minimum age for dextral shear

177 initiation: ~23 Ma in North Ayilari and ~19 Ma in Tangtse. The temperature of  
178 deformation recorded in the KKF outcrops in North Ayilari and Tangtse are higher  
179 than 450°C, implying that the Ar mica ages are cooling ages, which cannot be  
180 used to date the onset of right-lateral movement on the fault. The Lower Cenozoic  
181 granodiorite rocks found across the KKF, the YZ ophiolites and the GCT cannot  
182 be used to define accurate piercing points adequate to pin down the total offset on  
183 the KKF.

184 We conclude that the ~20 Ma magmatism along the KKF is synkinematic  
185 and that slip-rates, total offset and initiation age of movement on the fault are all  
186 significantly larger than those proposed by Wang et al. [2012]. More generally,  
187 this discussion illustrates the way, and the pitfalls that must be avoided, to define  
188 piercing points and date deformation on large continental strike-slip shear zones.  
189 Finally, while some distributed faulting and block rotation occurs in Tibet, there  
190 can be no doubt that the KKF is one of the main, long-lived, block-boundary faults  
191 in the India/Asia collision zone.

192

---

## 193 References

- 194 Boutonnet, E., et al. (2012), Synkinematic magmatism, heterogeneous deformation, and  
195 progressive strain localization in a strike-slip shear zone. The case of the right-lateral  
196 Karakorum fault, *Tectonics*, 31.
- 197 Chevalier, M.-L., et al. (2005), Response to comment on "Slip-rate measurements on the  
198 Karakorum fault may imply secular variations in fault motion". *Science*, 309, 1326.
- 199 Chevalier, M.-L., et al. (2012), Spatially constant slip rate along the southern segment of the  
200 Karakorum fault since 200 ka, *Tectonophysics*, 530/531, 152-179.
- 201 Hasalova, P., et al. (2011), Microstructural evidence for magma confluence and reusage of  
202 magma pathways: implications for magma hybridization, Karakoram Shear Zone in NW  
203 India, *J. Metamorph. Geol.*
- 204 Ji, W.-Q., et al. (2009), Zircon U–Pb geochronology and Hf isotopic constraints on petrogenesis  
205 of the Gangdese batholith, southern Tibet, *Chem. Geol.*, 262, 229-245.
- 206 Lacassin, R., et al. (2004a), Reply to Comment on large-scale geometry, offset and kinematic  
207 evolution of the Karakorum fault, TibetQ, *Earth Planet. Sci. Lett.*, 229, 159- 163.
- 208 Lacassin, R., et al. (2004b), Large-scale geometry, offset and kinematic evolution of the  
209 Karakorum fault, Tibet, *Earth Planet. Sci. Lett.*, 219, 255-269.
- 210 Leloup, P. H., et al. (2011), Long-lasting intracontinental strike-slip faulting: new evidence from  
211 the Karakorum shear zone in the Himalayas, *Terra Nova*, 23, 92-99.
- 212 Mukherjee, B. K., et al. (2012), Exhumation history of the Karakoram fault zone mylonites:  
213 New constraints from microstructures, fluid inclusions, and <sup>40</sup>Ar -<sup>39</sup>Ar analyses,



- 214 *Lithosphere*, 4, 230-241.
- 215 Murphy, M., et al. (2000), Southward propagation of the Karakoram fault system, Southwest  
216 Tibet; timing and magnitude of slip, *Geology*, 28, 451- 454.
- 217 Peltzer, G., and P. Tapponnier (1988), Formation and evolution of strike-slip faults, rifts, and  
218 basins during the India-Asia collision: an experimental approach, *J. Geophys. Res.*, 93,  
219 15,085 – 015,117.
- 220 Reichardt, H., et al. (2010), Hybridization of granitic magmas in the source: the origin of the  
221 Karakoram Batholith, Ladakh, NW India, *Lithos*, 116, 249-272.
- 222 Robinson, A. (2009), Geologic offsets across the northern Karakorum fault: Implications for its  
223 role and terrane correlations in the western Himalayan-Tibetan orogen, *Earth Planet. Sci.*  
224 *Lett.*
- 225 Searle, M. P. (1996), Geological evidence against large-scale pre-Holocene offsets along the  
226 Karakorum Fault: implications for the limited extrusion of the Tibetan plateau, *Tectonics*, 15,  
227 171-186.
- 228 Searle, M. P., and R. J. Phillips (2007), Relationships between right-lateral shear along the  
229 Karakoram fault and metamorphism, magmatism, exhumation and uplift: evidence from the  
230 K2–Gasherbrum–Pangong ranges, north Pakistan and Ladakh, *J. Geol. Soc. London*, 164,  
231 439–450.
- 232 Valli, F., et al. (2008), New U-Th/Pb constraints on timing of shearing and long-term slip-rate  
233 on the Karakorum fault, *Tectonics*, 27.
- 234 Wang, S., et al. (2012), Displacement along the Karakoram fault, NW Himalaya, estimated from  
235 LA-ICP-MS U–Pb dating of offset geologic markers, *Earth Planet. Sci. Lett.*, 337-338, 156-  
236 163.
- 237 Weinberg, R. F., et al. (2009), Magma ponding in the Karakoram shear zone, Ladakh, NW  
238 India, *Geol. Soc. Am. Bull.*, 121, 278-285.

239  
240  
241 **Figure 1.** Examples of published evidence for synkinematic melting along the  
242 KKF. (a) Leucocratic dyke P8 that crosscuts the right-lateral N130°-trending  
243 foliation, but exhibits two asymmetric tails indicative of NW-SE ductile right-  
244 lateral shear. The intrusive contact is underlined by red short dashes and the  
245 foliation by yellow long dashes. Oblique view from above. (b) Detail of one of the  
246 ductile tails of P8 showing cross-cutting relationship (intrusive, red short dashes)  
247 with the amphibolitic schists, and concordant contact with the marbles lying  
248 parallel to the main shearing direction. View from above, with a hammer for scale.  
249 (a) and (b) are from the Tangtse strand of the KKF [Boutonnet et al., 2012]. (c)  
250 Pegmatitic dyke LA58, stretched and boudinaged parallel to the right-lateral  
251 foliation (N135°/vertical, lineation pitch of 5 SE). The black frame corresponds to  
252 Figure 1d. (d) Detail of LA58, showing the schist layers embedded in the  
253 pegmatite as well as the right-lateral deformation (red arrows). (top) Field picture

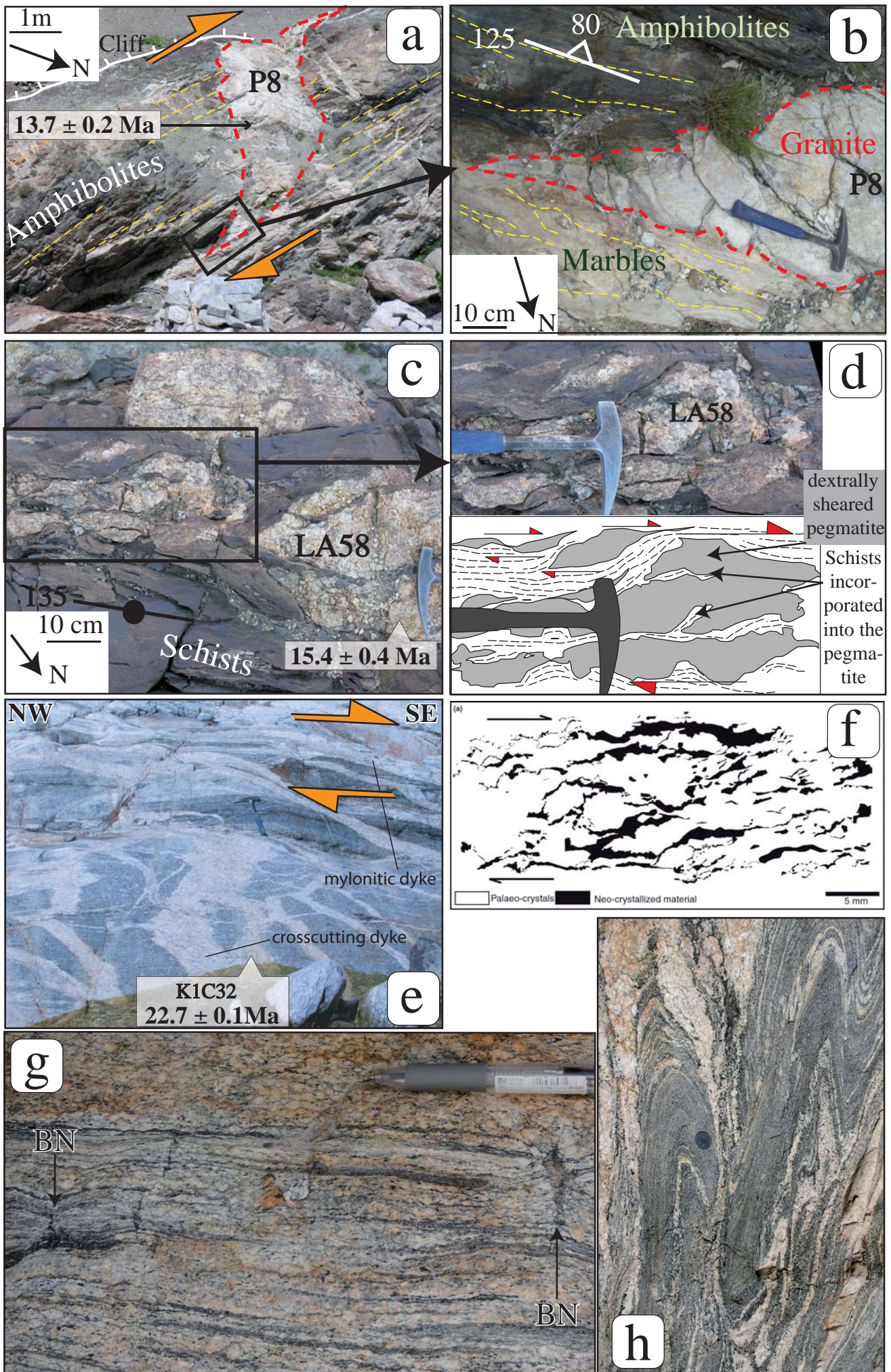
254 taken from above, (bottom) interpretative sketch. (c & d) are from the Muglib  
255 strand of the KKF [Boutonnet *et al.*, 2012]. (e) Cross-cutting veins in the  
256 foreground are intensely right-laterally sheared in the background. North Ayilari  
257 range [Valli *et al.*, 2008]. (f) Thin section map showing the distribution of neo-  
258 crystallized material at micro-scale (sample TNG165, Muglib strand of the KKF).  
259 The neo-crystallized material forms an interlinked extensive network broadly  
260 defining a right-lateral S-C fabric indicative of syn-magmatic shearing [Hasalova  
261 *et al.*, 2011]. (g) Accumulation of mica-rich melt in boudin necks (BN) of the  
262 deformed Ladakh granite indicating *in situ* partial melting during right-lateral  
263 deformation [Mukherjee *et al.*, 2012]. Tangtse strand of the KKF, view from  
264 above. (h) Deformed migmatites from the Tangtse gorge. View towards the NW,  
265 nearly vertical outcrop with a coin for scale. The fold axial planes are sub-parallel  
266 to the right-lateral shear of the KKF. The axial planar leucosomes, accommodating  
267 disruption and small slip of the antiform and synform, indicate syn-anatectic  
268 folding. Folds are part of dextral transpression on the KKF. The preferential  
269 preservation of antiforms and destruction of synforms is typical of deformation  
270 during partial melting.

271  
272 **Figure A1. Simplified geologic map of the Karakorum fault between 79°30'E**  
273 **and 82°E.**

274 Active faults drawn from Chevalier *et al.* [2012] and Valli *et al.* [2007]. The  
275 ophiolites and ophiolitic melanges as well as the other faults are drawn from the  
276 1/250 000 geologic maps. The KKF trace inferred by Wang *et al.* [2012] (green  
277 short dashes) cuts across the ophiolitic melange ignoring several fault branches.  
278 The northern boundary of the KKF zone (green long dashes) follows the northern  
279 edge of the suture zone north of Menci.

280 Kmz files of the active faults (ActiveFaults.kml) and the other faults (Faults.kml)  
281 are provided as supplementary material.

Figure  
Click here to download Figure: Figure1-commentWang.eps.pdf



**Supplementary material for on-line publication only**

[Click here to download Supplementary material for on-line publication only: FigA1.pdf](#)

**KML File (for GoogleMaps)**

[Click here to download KML File \(for GoogleMaps\): ActiveFaults.kml](#)

**KML File (for GoogleMaps)**

[Click here to download KML File \(for GoogleMaps\): Faults.kml](#)